3814 J. Phys. Chem. A 2002, 106, 3814−3818

Theoretical Study on the Mechanism of the CH + CH_3OH Reaction

Xiu-bin Zhang, Jian-jun Liu, Ze-sheng Li,* Jing-yao Liu, and Chia-chung Sun

Institute of Theoretical Chemistry, State Key Laboratory of Theoretical and Computational Chemistry, Jilin University, Changchun 130023, P. R. China

Received: December 18, 2001; In Final Form: February 8, 2002

The possible reaction mechanism of CH radical with CH_3OH is investigated theoretically by a detailed potential energy surface calculation at the B3LYP/6-311G(d,p) and CCSD(T)/6-311+G(d,p) (single-point) levels. Various possible reaction paths including three kinds of insertion reaction and two kinds of H-abstraction reactions are considered. Among them, the most feasible pathway should be a CH radical attacking on the lone pair of the oxygen atom in CH_3OH to form the anti C−O complex $\mathbf{a_1}$, followed by a CH inserting into the O−H bond to form the low-lying methoxymethyl radical $\mathbf{a_3}$. Starting from $\mathbf{a_3}$, the most competitive reaction pathway is the direct C−O single bond fission leading to the product $\mathbf{P_1}$ $CH_2O + CH_3$. The other reaction pathways are less competitive due to thermodynamical or kinetic factors. Furthermore, our calculation results show that, in terms of potential energy surface, the title reaction involves all the main features of both CH + H_2O and CH + CH_4 reactions; however, the reaction mechanism of CH with CH_3OH may be more similar to that of CH + H_2O. Our results may be helpful for understanding the mechanism of a CH radical insertion reaction.

1. Introduction

As one of the most reactive radicals, methylidyne (CH) is important in combustion and planetary atmospheric chemistry. The reactions of the CH radical with numerous small molecules have been studied experimentally and theoretically.[1−12] For the reactions of CH with CH_4, NH_3, H_2O, and HF, several theoretical studies have shown that the insertion reaction pathway is the dominant channel, whereas the direct H-abstraction reactions are less competitive due to the weak endothermicity.[7−9] The calculated results are in agreement with kinetic experiments.[10−12] Particularly, it should be pointed out that, as there was no lone pair in the carbon atom of CH_4, the mechanism for the CH + CH_4 insertion reaction was found to be different from that of the other three insertion reactions, but somewhat similar to that of the $CH_2 + CH_4$ insertion reaction.[7] Note that methanol has dual features of both CH_4 and H_2O, so the reaction of CH with CH_3OH may proceed via the following: (1) the direct H-abstraction leading to $CH_3O + CH_2$ (similar to the abstraction reaction of CH with H_2O); (2) the direct H-abstraction to form $CH_2OH + CH_2$ (similar to the abstraction reaction of CH with CH_4); (3) forming an intermediate C−C complex and then a CH radical inserting into the C−H bond in CH_3OH (similar to the insertion reaction of CH with CH_4). (4) CH radical attacking on the lone pair of the oxygen in CH_3OH to form an initial C−O complex followed by CH inserting into the O−H (similar to the insertion reaction of CH with H_2O), or CH inserting into the C−O bond in CH_3OH. Thus, it seems necessary to determine which pathway is more favorable for the title reaction. In addition, the reaction of CH with methanol is of practical relevance, for methanol can be used as an alternative fuel, which has lower pollution potential and can be produced from biomass.[13,14] So the reaction of CH with CH_3OH is worthy of being studied theoretically.

Recently, the reactions of the CH radical with a variety of methanol isotopomers were studied by using pulsed laser photolysis/laser-induced fluorescence, as a function of temperature (298−753 K) and pressure (100−600 Torr helium).[15] The rate constant of the title reaction was measured to be $k = (2.52 \pm 0.12) \times 10^{-10}$ cm^3 molecule^{-1} s^{-1} at 298 K, which was independent of total pressure. In the experiment, the possibility of the CH radical inserting into a C−H bond in CH_3OH was excluded considering the absence of any significant isotope effect. It was found that the title reaction proceeds via an initial complex with the subsequent insertion of CH into either the O−H or the C−O bond.[15] Since the CH radical may insert into the C−O or O−H bond, which pathway is more favorable? In addition, though in the experiment some products are assumed based on the thermodynamic data, such an intuitive guess needs to be confirmed, just as Johnson et al. stated that “Further analysis is hindered by a lack of knowledge of the transition states for such barrierless insertion reactions” for the CH + CH_3OH reaction.[15] To our best knowledge, there is not any theoretical study on this important reaction up to now. Therefore, in this paper, a detailed theoretical investigation on the whole potential energy surface of the title reaction is performed, and the results may be helpful to resolve the puzzle mentioned above.

2. Computational Methods

All computations are carried out with the Gaussian 98 program package.[16] Full geometry optimization is performed at the B3LYP/6-311G(d, p) level along with analytic vibrational frequency calculations in order to characterize the obtained structures as minima or as transition states on the potential energy surface. Moreover, single-point energies are calculated at the CCSD(T)/6-311+G(d,p) level using the B3LYP/6-311G(d,p)-optimized geometries. To test whether the transition state corresponds to the right isomers, the intrinsic reaction coordinate (IRC) calculations are also performed at the B3LYP/6-311G(d, p) level. The CCSD(T) single-point energies are used in the following discussions unless otherwise noted.

---

* Author to whom correspondence should be addressed.

10.1021/jp014602w CCC: $22.00

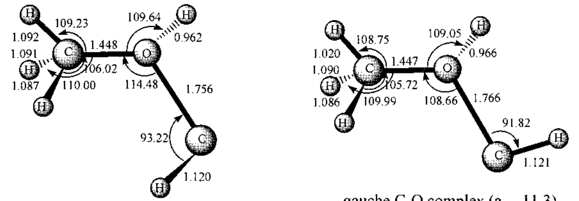

anti C-O complex (a_1, -11.4)

gauche C-O complex (a_2, -11.3)

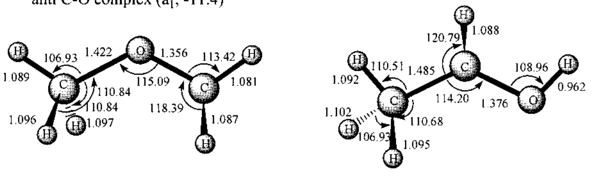

methoxymethyl radical (a_3, -87.3)

gauche-1-methoxyethyl radical (b_1, -100.9)

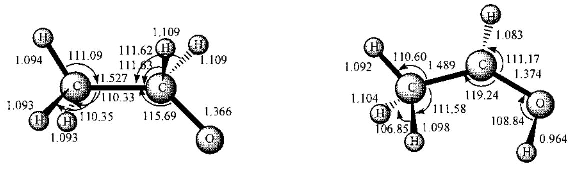

ethoxy radical (b_2, -92.7)

anti-1-methoxyethyl radical (b_3, -100.6)

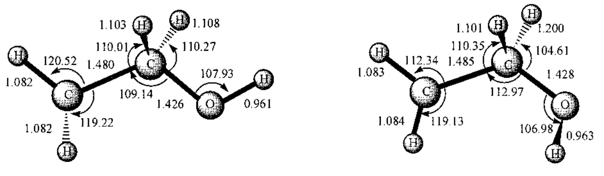

gauche-2-methoxy radical (b_4, -93.6)

anti-2-methoxy radical (b_5, -94.2)

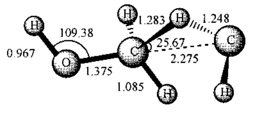

C-C complex (b_6, -3.6)

Figure 1. The B3LYP/6-311G(d, p)-optimized geometries of all complexes and isomers. Bond distance is in angstrom and angle in degree. The values in parentheses are the CCSD(T) + ZPE relative energies

3. Results and Discussions

For the present C_2H_5O system, three intermediate complexes, six intermediate isomers, and seventeen transition states are obtained. The structures of the complexes and isomers are depicted in Figure 1, where a_n ($n = 1, 2, 3$) and b_n ($n = 1, 2, ..., 6$) are the corresponding labels, a and b are used to represent COC and CCO skeletons, respectively. Figure 2 shows the structures of the transition states, in which the symbol **TSxy** is used to denote a transition state, **x** and **y** are the corresponding isomers or products. The values in parentheses of Figure 1 and Figure 2 are the CCSD(T)+ZPE relative energies. The energetic data of various products, complexes and isomers, and transition states are listed in Table 1, Table 2, and Table 3, respectively. It should be noted that the energy of CH + CH_3OH is set at zero as a reference for other species. As shown in Table 1, our calculated relative energies for the products are in agreement with the experimental reaction heats of the products.[8] By means of the interrelation among the reactants, isomers, transition states, and products as well as the corresponding relative energies, the schematic profiles of the potential energy surface are depicted as shown in Figure 3, where the values in parentheses are the CCSD(T) + ZPE relative energies.

The following discussions are organized as follows. In section 3.1, five possible association pathways of CH attacking on CH_3OH are compared and the most feasible one is determined. Then in section 3.2, the reaction mechanism after the insertion reactions is discussed. Finally in section 3.3, we will compare our calculated results with those of experiments.

3.1. Initial Associations. As mentioned in the Introduction, the attack of a CH radical on a CH_3OH molecule may have several possible ways. First, product $\mathbf{P_8}$ $CH_3O + {}^3CH_2$ can be formed via the direct inter-H-shift from the O-atom in CH_3OH to C-atom in CH. However, $\mathbf{P_8}$ lies 2.0 kcal/mol higher than the reactants **R** CH + CH_3OH. Therefore, the formation of $\mathbf{P_8}$ is thermodynamically unfavorable compared with other products. Second, the inter-H-shift from the C-atom in CH_3OH to the C-atom in CH leads to product $\mathbf{P_7}$ $CH_2OH + {}^3CH_2$. It should be pointed out that at the HF/6-311G(d,p) level, we obtain the transition state $\mathbf{TSRP_7}$, but the attempt to obtain the transition state at the higher levels of B3LYP/6-311G(d,p) and MP2/6-311G(d,p) failed. The CCSD(T)/6-311+G(d.p) single-point calculation for the HF-optimized geometry shows that $\mathbf{TSRP_7}$ lies 0.5 kcal/mol above the reactants **R**. Thus the direct inter-H-shift from the C-atom in CH_3OH to the C-atom in CH may be dynamically unfeasible and may play a part role at medium high temperatures. Third, in an analogous way with the insertion reaction of CH with CH_4, the intermediate C−C complex ($\mathbf{b_6}$) (as shown in Figure 1) is first formed, which is only 3.6 kcal/mol lower than that of the reactants and involves a very low vibrational frequency of 48 cm^{-1}, corresponding to the stretch of the C−O bond. This means that the C−C complex $\mathbf{b_6}$ is unstable. After the formation of $\mathbf{b_6}$, the CH radical can insert into the C−H bond in CH_3OH to give the anti 2-methoxy radical ($\mathbf{b_5}$). Such a process can be represented as $\mathbf{R} \rightarrow \mathbf{b_6} \rightarrow \mathbf{b_5}$ (see Figure 3). The transition state $\mathbf{TSb_6b_5}$ lies 1.1 kcal/mol below the reactants and thus such a reaction pathway may be feasible. It should be noted that this reaction pathway can be determined only at the B3LYP/6-31G(d,p) level. At the higher level of B3LYP/6-311G(d,p), our attempt to locate the intermediate complex $HCCH_3OH$ $\mathbf{b_6}$ and the transition state $\mathbf{TSb_6b_5}$ failed. Finally, let us discuss the other two insertion reaction paths. Starting from the reactants **R**, by the CH radical attacking on the lone pair of the oxygen, the anti C−O complex ($\mathbf{a_1}$) and the gauche C−O complex ($\mathbf{a_2}$) (as shown in Figure 1) with relative energies of −11.4 and −11.3 kcal/mol, respectively, can be first formed with no barrier. Then, the CH radical in $\mathbf{a_1}$ inserts into the O−H bond to form the low-lying methoxymethyl radical ($\mathbf{a_3}$) via $\mathbf{TSa_1a_3}$, while the CH in $\mathbf{a_2}$ inserts into the C−O bond leading to the lowest-lying ethoxy radical ($\mathbf{b_1}$) through $\mathbf{TSa_2b_1}$. Comparing the relative energies of the two transition states as shown in Table 3, it is found that $\mathbf{TSa_1a_3}$ is 2.5 kcal/mol lower than the reactants, contrarily, $\mathbf{TSa_2b_1}$ is 23.8 kcal/mol higher than the reactants. So the reaction pathway of CH inserting into the O−H bond ($\mathbf{R} \rightarrow \mathbf{a_1} \rightarrow \mathbf{a_3}$) is more feasible, whereas CH insertion into the C−O bond ($\mathbf{R} \rightarrow \mathbf{a_2} \rightarrow \mathbf{b_1}$) is kinetically unfavorable. Interestingly, from our calculations it is found that $\mathbf{b_1}$ can be obtained from $\mathbf{a_3}$ via the H-shift succeeding the CH_3-shift process. Such a reaction pathway can be written as $\mathbf{R} \rightarrow \mathbf{a_1} \rightarrow \mathbf{a_3} \rightarrow \mathbf{b_2} \rightarrow \mathbf{b_1}$. As shown in Figure 3, all transition states in this pathway lie below the reactants, whereas $\mathbf{R} \rightarrow \mathbf{a_2} \rightarrow \mathbf{b_1}$ involves a high-lying transition state $\mathbf{TSa_2b_1}$ (23.8 kcal/mol). So, $\mathbf{R} \rightarrow \mathbf{a_1} \rightarrow \mathbf{a_3} \rightarrow \mathbf{b_2} \rightarrow \mathbf{b_1}$ is more feasible than $\mathbf{R} \rightarrow \mathbf{a_2} \rightarrow \mathbf{b_1}$.

As discussed above, only two attack ways of CH are kinetically feasible for the reaction of CH with CH_3OH, i.e., the CH radical inserting into the C−H bond to give the anti 2-methoxy radical ($\mathbf{b_5}$) ($\mathbf{R} \rightarrow \mathbf{b_6} \rightarrow \mathbf{b_5}$) or inserting into the O−H bond to form methoxymethyl radical $\mathbf{a_3}$ ($\mathbf{R} \rightarrow \mathbf{a_1} \rightarrow \mathbf{a_3}$). Now let us compare the feasibility of the two pathways. Energetically,

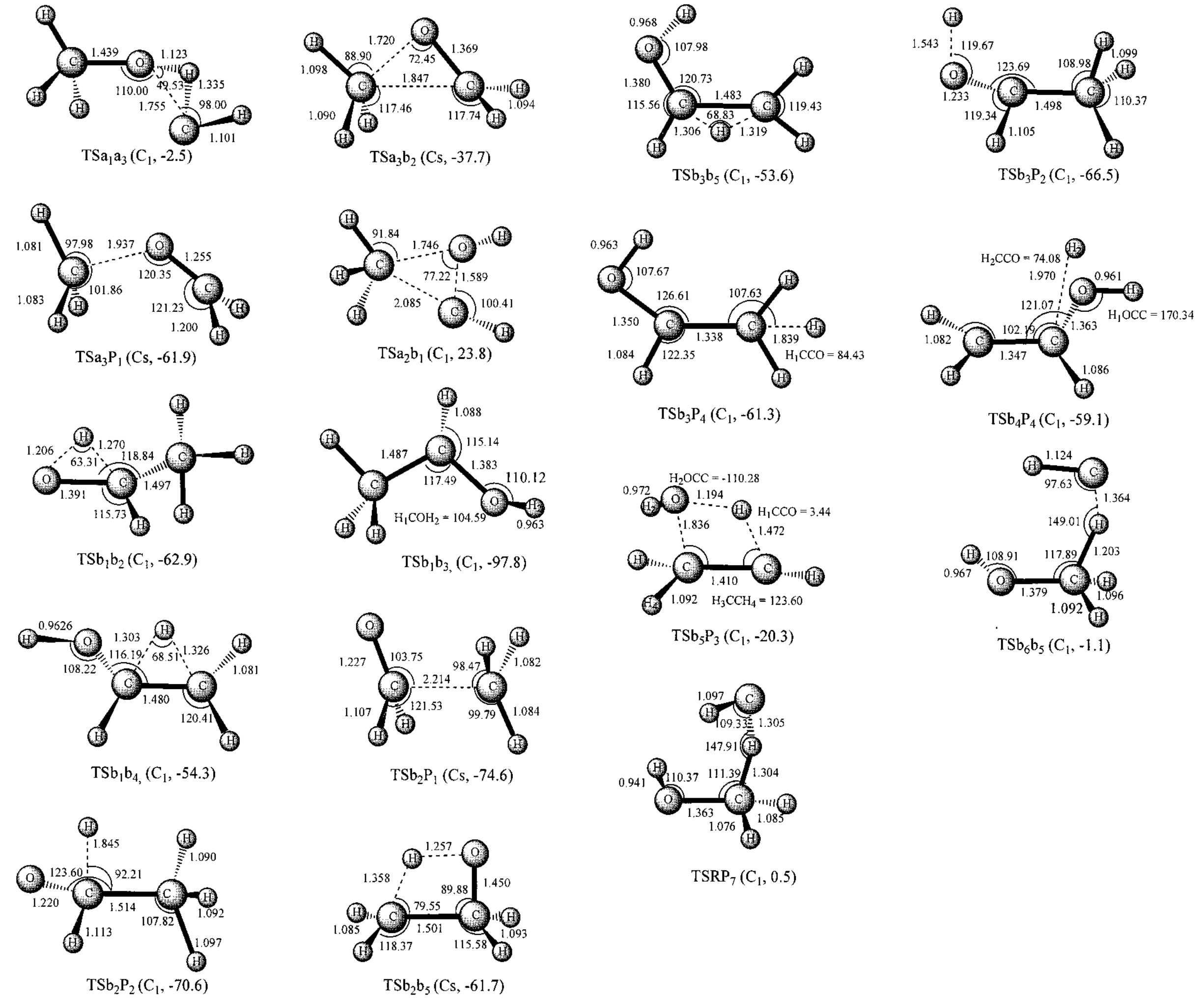

Figure 2. The B3LYP/6-311G(d, p)-optimized geometries of all transition states. Bond distance is in angstrom and angle in degree. The values in parentheses are the CCSD(T) + ZPE relative energies

TABLE 1: Zero-Point, Total (a.u.), and Relative Energies in Parentheses (kcal/mol) as Well as Those Including Zero-Point Vibration Energies (kcal/mol) of the Reactant and Products for the $CH_3OH + CH$ Reaction

species	ZPE	B3LYP	CCSD(T)	CCSD(T) + ZPE	experimental reaction heats
R $CH_3OH + CH$	0.057504	−154.229371 (0.0)	−153.868254 (0.0)	0.0	
P_1 $CH_2O + CH_3$	0.056054	−154.390098 (−100.9)	−153.999982 (−82.7)	−83.6	−85.1
P_2 $CH_3CHO + H$	0.055211	−154.379017 (−93.9)	−153.991654 (−77.4)	−78.9	−81.7
P_3 $CH_2CH + H_2O$	0.057640	−154.374480 (−91.1)	−153.989759 (−76.2)	−76.2	
P_4 $CH_2CH_2 + OH$	0.059240	−154.368505 (−87.3)	−153.981754 (−71.2)	−70.1	−72.2
P_5 $CH_2CHOH + H$	0.056506	−154.361846 (−83.1)	−153.972975 (−65.7)	−66.3	
P_6 $CH_3CH_2 + O$	0.058938	−154.269021 (−24.9)	−153.886289 (−11.3)	−10.4	−5.9
P_7 $CH_2OH + {}^3CH_2$	0.053274	−154.259559 (−18.9)	−153.872522 (−2.6)	−5.3	
P_8 $CH_3O + {}^3CH_2$	0.053439	−154.25093 (−13.5)	−153.861021 (4.5)	2.0	3.6

C−C complex $\mathbf{b_6}$ is only 3.6 kcal/mol lower than the reactants **R**, thus it is readily dissociated to the reactants, whereas the anti C−O complex $\mathbf{a_1}$ with the relative energy of −11.4 kcal/mol is more stable. In addition, the CH may attack more easily on the O-atom than the C-atom in CH_3OH because the O-atom with a lone pair strongly attracts the CH radical. As a result, the most feasible association way should be the CH radical attacking on the lone pair of the oxygen to form the initial anti C−O complex $\mathbf{a_1}$ followed by the CH inserting into the O−H bond to form $\mathbf{a_3}$. In the following discussions, we will mainly focus on the reaction pathways starting from the methoxymethyl radical $\mathbf{a_3}$.

3.2. Reaction Mechanism. As shown in Figure 3, there are three possible reaction pathways from isomer $\mathbf{a_3}$. First, $\mathbf{a_3}$ can directly dissociate to high-lying product $\mathbf{P_7}$ $CH_2OH + {}^3CH_2$ (2.0 kcal/mol) through the C−O single bond cleavage. For this process, a well-defined transition state cannot be located. In terms of the total reaction, the formation of $\mathbf{P_7}$ requires endothermicity and thus is thermodynamically unfavorable. Second, $\mathbf{a_3}$ can isomerize to the ethoxy radical $\mathbf{b_2}$ via a CH_3-shift transition state $\mathbf{TSa_3b_2}$. However, the barrier of 49.6 kcal/mol is needed to overcome for this isomerization process. Third, the most competitive pathway from $\mathbf{a_3}$ should be C−O bond fission leading to $\mathbf{P_1}$ via the transition state $\mathbf{TSa_3P_1}$. Such a process only requires surmounting the barrier of 25.4 kcal/mol.

Furthermore, some products including $\mathbf{P_2}$ $CH_3CHO + H$, $\mathbf{P_3}$ $CH_2CH + H_2O$, $\mathbf{P_4}$ $CH_2CH_2 + OH$, $\mathbf{P_5}$ $CH_2CHOH + H$, and $\mathbf{P_6}$ $CH_3CH_2 + O$, which play an important role in organic

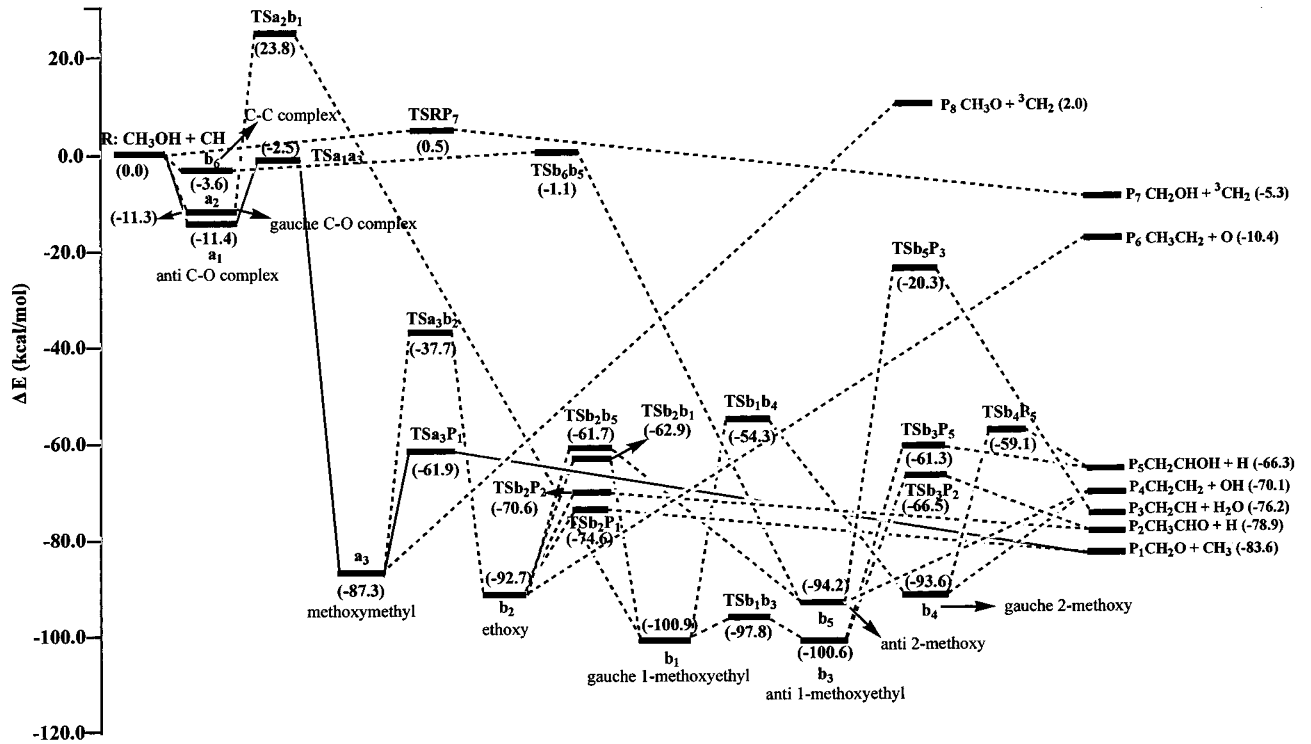

Figure 3. The potential energy surface of the CH + CH$_3$OH reaction. The values in parentheses are the CCSD(T) + ZPE relative energies.

TABLE 2: Zero-Point, Total (a.u.), and Relative Energies in Parentheses (kcal/mol) as Well as Those Including Zero-Point Vibration Energies (kcal/mol) of Complexes and Intermediate Isomers for the CH$_3$OH + CH Reaction

species	ZPE	B3LYP	CCSD(T)	CCSD(T) + ZPE (−15.2)
anti C−O complex (a$_1$)	0.063565	−154.282341 (−33.2)	−153.892467	−11.4
gauche C−O complex (a$_2$)	0.063262	−154.281267 (−32.6)	−153.891992 (−14.9)	−11.3
methoxymethyl (a$_3$)	0.065516	−154.409427 (−113.0)	−154.015370 (−92.3)	−87.3
gauche 1-methoxyethyl (b$_1$)	0.065800	−154.429213 (−125.4)	−154.037412 (−106.1)	−100.9
ethoxy (b$_2$)	0.063969	−154.417060 (−117.8)	−154.0229130 (−97.0)	−92.7
anti 1-methoxyethyl (b$_3$)	0.065847	−154.428904 (−125.2)	−154.036853 (−105.8)	−100.6
gauche 2-methoxy (b$_4$)	0.064299	−154.412910 (−115.2)	−154.024246 (−97.9)	−93.6
anti 2-methoxy (b$_5$)	0.065059	−154.415298 (−116.7)	−154.025994 (−99.0)	−94.2
C−C complex (b$_6$)	0.059255	−154.2215595 (B3LYP/6−31 g**)	153.875788 (−4.7)	−3.6

TABLE 3: Zero-point, Total (a.u.) and Relative Energies in Parentheses (kcal/mol) as Well as Those Including Zero-point Vibration Energies (kcal/mol) of the Transition States for the CH$_3$OH + CH Reaction

species	ZPE	B3LYP	CCSD(T)	CCSD(T) + ZPE
TSa$_1$a$_3$	0.058642	−154.266967 (−23.6)	−153.873422 (−3.2)	−2.5
Tsa$_2$b$_1$	0.061311	−154.230512 (−0.7)	−153.834123 (21.4)	23.8
Tsa$_3$b$_2$	0.062551	−154.328301 (−62.1)	−153.933423 (−40.9)	−37.7
Tsa$_3$P$_1$	0.060017	−154.369994 (−88.2)	−153.969442 (−63.5)	−61.9
TSb$_1$b$_2$	0.060736	−154.365838 (−85.6)	−153.971769 (−65.0)	−62.9
TSb$_1$b$_4$	0.060970	−154.351503 (−76.6)	−153.958264 (−56.5)	−54.3
TSb$_1$b$_3$	0.064121	−154.422218 (−121.0)	−154.030731 (−102.0)	−97.8
TSb$_2$P$_1$	0.060759	−154.385483 (−98.0)	−153.990457 (−76.7)	−74.6
TSb$_2$P$_2$	0.056860	−154.372680 (−89.9)	−153.980119 (−70.2)	−70.6
TSb$_2$b$_5$	0.061326	−154.364469 (−84.8)	−153.970333 (−64.1)	−61.67
TSb$_3$b$_5$	0.060509	−154.350654 (−76.1)	−153.956634 (−55.5)	−53.6
TSb$_3$P$_2$	0.056319	−154.369879 (−88.2)	−153.973015 (−65.7)	−66.5
TSb$_3$P$_4$	0.060056	−154.441353 (−133.0)	−153.968439 (−62.9)	−61.3
TSb$_4$P$_4$	0.057716	−154.356877 (−80.0)	−153.962796 (−59.3)	−59.1
TSb$_5$P$_3$	0.057350	−154.297244 (−42.6)	−153.900412 (−20.2)	−20.3
TSb$_6$b$_5$	0.059192	−154.2182515 (B3LYP/6−31 g**)	−153.871632 (−2.1)	(−1.1)
TSRP$_7$	0.059530	−153.333176 (HF/6−311G**)	−153.869440 (−0.7)	(0.5)

chemistry and combustion process, also can be obtained via the dissociation of the C−C−O frame isomers (labeled as **b**). As shown in Figure 3, there are three reaction pathways leading to these isomers, i.e., **R** → **a$_2$** → **b$_1$**, **R** → **b$_6$** → **b$_5$**, and **R** → **a$_1$** → **a$_3$** → **b$_2$**. As discussed in section 3.1, the former two reaction pathways cannot compete with **R** → **a$_1$** → **a$_3$**. For **R** → **a$_1$** → **a$_3$** → **b$_2$**, the conversion transition state **TSa$_3$b$_2$** lies 24.2 kcal/mol higher than **TSa$_3$P$_1$** in **R** → **a$_1$** → **a$_3$** → **P$_1$**. So **R** → **a$_1$** → **a$_3$** is the most competitive. Consequently, reflected in the final product distribution, we may predict that **P$_1$** is the most feasible product and the other products **P$_2$**−**P$_6$** cannot compete with **P$_1$**.

To give a deeper understanding of the reaction mechanism of CH + CH$_3$OH, it is worthwhile to compare the title reaction with two analogous reactions CH + H$_2$O and CH + CH$_4$. The two reactions have been extensively studied experimentally and theoretically.[7−12] Theoretical calculations show that they exist in similarity and discrepancy.[7,8] The similarity of the two reactions is that the insertion reaction is energetically favorable, while the H-abstraction reaction cannot compete with it. Such a conclusion is in good agreement with experimental observations.[10−12] The discrepancy lies in the formation of complexes before the insertion reaction. For CH + H_2O reaction, the CH attacks the lone pair electrons in the O-atom followed by the formation of a very stable donor−acceptor complex. For the CH + CH_4 reaction, only an unstable weak bond complex is formed. For the title reaction of CH with CH_3OH, five possible attack ways are considered in the present study. The most feasible reaction pathway is the attack of CH on the lone pair of the O-atom leading to the stable anti C−O complex $\mathbf{a_1}$ followed by CH inserting into the O−H bond to form the low-lying methoxymethyl radical $\mathbf{a_3}$, Subsequently, $\mathbf{a_3}$ directly dissociates to $\mathbf{P_1}$ CH_3 + OCH_2. The second competitive attack way is the formation of the unstable weak bond C−C complex $\mathbf{b_6}$ and then CH inserting into the C−H bond to form the lowest-lying anti 2-methoxy radical $\mathbf{b_5}$. It is obvious that the reaction of CH with CH_3OH involves all the main features of CH + H_2O and CH + CH_4 reactions. However, from the discussions above, it is found that the reaction mechanism of CH + CH_3OH is more similar to that of CH + H_2O.

As an extrapolation, let us give a prediction of the other similar reaction CH + CH_3OCH_3 which is not studied both experimentally and theoretically as yet. In this reaction, three attack ways may be included: (1) the attack of CH on an O-atom to form the initial complex followed by inserting into the C−O bond; (2) the formation of the weak bond complex and then insertion of CH into the C−H bond in CH_3OCH_3; (3) the direct H-abstraction to form CH_2OCH_3 + CH_2. According to the discussions in section 3.1, the second pathway may be the most favorable, so it seems reasonable to assume that CH + CH_3OCH_3 may be related more closely to CH + CH_4 than to CH + H_2O.

3.3. Experimental Implication. Recently, Johnson et. al. carried out the kinetic study for the title reaction.[15] In their experiment, they excluded the feasibility of the insertion of CH into the C−H bond in CH_3OH, and suggested that the feasible association ways were the attack of CH on the O-atom in CH_3OH to form the initial complex and the subsequent insertion into either the C−O bond or O−H bond to form $HOCHCH_3$ or CH_2OCH_3, respectively. They also assumed that $HOCHCH_3$ and CH_2OCH_3 could dissociate to CH_3CHO + H and CH_2O + CH_3, respectively. They did not predict that which insertion way is more favorable and which product is the most competitive. In our calculations, it is shown that among the five possible association ways, the most feasible one is the attack of CH on the O-atom in CH_3OH to form the initial complex before CH insertion into the C−O bond or O−H bond. Furthermore, it is found that the most feasible reaction pathways should be the insertion of CH into the O−H bond in CH_3OH leading to methoxymethyl radical $\mathbf{a_3}$ followed by its dissociation to the most competitive $\mathbf{P_1}$ CH_2O + CH_3. The insertion of CH into the C−O bond in CH_3OH leading to gauche 1-methoxyethyl $\mathbf{b_1}$ is kinetically unfavorable since the transition state $\mathbf{TSa_2b_1}$ is 23.8 kcal/mol higher than the reactants **R**. However, our calculation shows that $\mathbf{b_1}$ can be obtained from another pathway, i.e., via the continual CH_3-shift and H-shift of $\mathbf{a_3}$.

Finally, it should be pointed out that for the title reaction all involved intermediates and transition states in the main reaction pathway $\mathbf{R} \rightarrow \mathbf{a_1} \rightarrow \mathbf{a_3} \rightarrow \mathbf{P_1}$ lie below the reactants. Once the insertion reaction proceeds, the reaction system immediately enters a deep potential well. Undoubtedly, these features will make the reaction faster. Therefore, the title reaction is expected to be very fast. This is qualitatively consistent with the experimental result.[15]

4. Conclusion

The theoretical study gives some insights into the mechanism of the reaction of CH radical with CH_3OH. Five possible attack ways are considered in the present study. The most feasible reaction pathway is the attack of CH on the lone pair of the O-atom leading to the stable anti C−O complex $\mathbf{a_1}$ followed by the insertion of CH into the O−H bond to form the low-lying intermediate methoxymethyl $\mathbf{a_3}$. Subsequently, $\mathbf{a_3}$ directly dissociates to $\mathbf{P_1}$ CH_2O + CH_3. The second competitive attack way is the formation of the unstable weak bond C−C complex $\mathbf{b_6}$ and then inserting into the C−H bond to form the lowest-lying anti 2-methoxy radical $\mathbf{b_5}$. It is shown that, in terms of the potential energy surface, the CH + CH_3OH reaction involves all the main features of CH + H_2O and CH + CH_4 reactions. Furthermore, it is found that the reaction mechanism of CH + CH_3OH is more similar to that of CH + H_2O.

Acknowledgment. This work is supported by the Natural Science Foundation of China (G29892168, 20073014, 20103003), Doctor Foundation by the Ministry of Education, Foundation for University Key Teacher by the Ministry of Education and Key Subject of Science and Technology by the Ministry of Education of China.

References and Notes

(1) Sanders W. A.; Lin M. C. In *Chemical kinetic of small organic radicals*; Vol. III. *Reactions of special radicals*. Z., Alfassi, Ed.; CRC Press: Boca Ration, FL, 1988.

(2) Aoyagi, M.; Shepard, R.; Wagner, A. F.; Dunning, T. H., Jr.; Brown, F. B. *J. Phys. Chem.* **1990**, *94*, 3236.

(3) Walch, S. P. *J. Chem. Phys.* **1995**, *103*, 7064.

(4) Martin, J. M. L.; Taylor, P. R. *Chem. Phys. Lett.* **1993**, *209*, 143.

(5) Walch, S. P. *Chem. Phys. Lett.* **1993**, *208*, 214.

(6) Manaa, M. R.; Yarkony, D. R. *J. Chem. Phys.* **1991**, *95*, 1808.

(7) Wang, Z. X, Hung, M. B.; Liu, R. Z. *Can. J. Chem.* **1997**, *75*, 996.

(8) Wang, Z. X.; Liu, R. Z.; Huang, M. B.; Yu, Z. H. *Can. J. Chem.* **1996**, *74*, 910.

(9) Berman, M. R.; Lin, M. C. *Chem. Phys.* **1983**, *82*, 435.

(10) (a) Zabarnick, S.; Fleming, J. W.; Lin, M. C. *Chem. Phys.* **1989**, *132*, 407. (b) Becker, K. H.; Engelhardt, B.; Geiger, H.; Kurtenbach, R.; Wissen, P. *Chem. Phys. Lett.* **1993**, *210*, 135.

(11) Zabarnick, S.; Fleming, J. W.; Lin, M. C. *Symp. (Int.) Combust. [Proc.] 21st*; The Combustion Institute: Pittsburgh, 1986; p 713.

(12) Jursic, B. S. *J. Phys. Chem. A* **199**8, *102*, 9255.

(13) Ohshita, S. B.; Seigneur, C. *J. Air Waste Manage. Assoc.* **1993**, *97*, 12275.

(14) Karaosmanoglu, F.; IsigigurErgudenler, A.; Aksoy, H. A. *Energy Sources* **1998**, *20*, 955.

(15) Johnson, D. G.; Blitz, M. A.; Seakins, P. W. *Phys. Chem. Chem. Phys.* **2000**, *2*, 2549.

(16) Frisch, M. J.; Trucks, G. W.; Schlegel, H. B.; Scuseria, G. E.; Robb, M. A.; Cheeseman, J. R.; Zakrzewski, V. G.; Montgomery, J. A., Jr.; Stratmann, R. E.; Burant, J. C.; Dapprich, S.; Millam, J. M.; Daniels, A. D.; Kudin, K. N.; Strain, M. C.; Farkas, O.; Tomasi, J.; Barone, V.; Cossi, M.; Cammi, R.; Mennucci, B.; Pomelli, C.; Adamo, C.; Clifford, S.; Ochterski, J.; Petersson, G. A.; Ayala, P. Y.; Cui, Q.; Morokuma, K.; Malick, D. K.; Rabuck, A. D.; Raghavachari, K.; Foresman, J. B.; Cioslowski, J.; Ortiz, J. V.; Stefanov, B. B.; Liu, G.; Liashenko, A.; Piskorz, P.; Komaromi, I.; Gomperts, R.; Martin, R. L.; Fox, D. J.; Keith, T.; Al-Laham, M. A.; Peng, C. Y.; Nanayakkara, A.; Gonzalez, C.; Challacombe, M.; Gill, P. M. W.; Johnson, B. G.; Chen, W.; Wong, M. W.; Andres, J. L.; Head-Gordon, M.; Replogle, E. S.; Pople, J. A. *Gaussian 98*, revision A.9; Gaussian, Inc.: Pittsburgh, PA, 1998.